Observational constraints on the dark energy density evolution

Michael Doran, Khamphee Karwan, and Christof Wetterich
Institut für Theoretische Physik, Universität Heidelberg,Philosophenweg 16, 69120 Heidelberg, Germany

We constrain the evolution of the dark energy density Ω_d from Cosmic Microwave Background, Large Scale Structure, and Supernovae Ia measurements. While Supernovae Ia are most sensitive to the equation of state w_0 of dark energy today, the Cosmic Microwave Background and Large Scale Structure data best constrains the dark energy evolution at earlier times. For the parametrization used in our models, we find $w_0 < -0.8$ and the dark energy fraction at very high redshift $\Omega_d^e < 0.03$ at 95 per cent confidence level.

PACS numbers: 98.80.-k

Observations [1, 2, 3, 4, 5, 6, 7] indicate that a mysterious form of dark energy [9, 10, 11, 12] is driving an accelerated expansion of our Universe. So far, the focus has been on the equation of state $w \equiv \bar{p}/\bar{\rho}$ of dark energy and in particular on its current value w_0. However, if a dynamical dark energy or quintessence arises from the time evolution of a scalar (cosmon) field one expects in general, that the equation of state changes as the Universe expands. Various parameterizations of w as a function of the scale factor a or redshift z have been investigated [13, 14, 15, 16] . Yet, it is rather the amount of dark energy Ω_d than the equation of state (which is related to the derivative of Ω_d) that influenced our Universe in the past. In this spirit, suitably averaged quantities like $\bar{\Omega}_{\rm ls}$ [17] and $\bar{\Omega}_{\rm sf}$ [18] have been used to describe the effects of dark energy at the time of last scattering and during structure formation.

No parameterization of w or Ω_d – no matter how complicated – will perfectly describe the evolution of dark energy. Yet, some essential key features for a viable model seem to be the following: today, the amount of dark energy should be $\sim 70\%$. Going back in time, this value must have decreased considerably, as current constraints yield a fraction of dark energy at the time of last scattering $\bar{\Omega}_{\rm ls} \lesssim 8\%$ [19]. Supernovae measurements tell us that this decrease must have occurred swiftly, as the slope of this decrease is reflected in $w_0 \lesssim -0.7$.

Usually, observations at low redshift, such as Sne Ia measurements are combined with structure formation and CMB observations that are probing earlier epochs. In this paper, we will take a different point of view. Given the uncertainties in parameterizing Ω_d or equivalently w, we look at high redshift and low redshift constraints separately. We use a particularly simple and direct parameterization of the dark energy evolution [20]. The parameters are the amount of dark energy today Ω_d^0 and the amount of dark energy at early times Ω_d^e to which it asymptotes for very large z. In terms of these, our parameterization is

$$\Omega_d(a) = \frac{e^R}{1+e^R}, \tag{1}$$

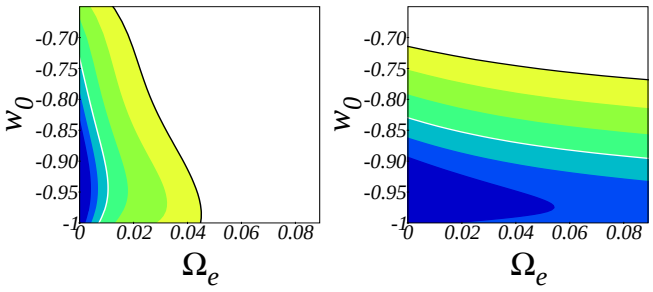

FIG. 1: Constraints on the model parameters Ω_d^e and w_0. The left panel depicts the distribution from WMAP+CBI+VSA+SDSS+HST data, the right panel that of Sne Ia alone. The regions of 68% (95%) are enclosed by a white (black) line. The two data sets give almost orthogonal information: Sne Ia constrain w_0 but are less sensitive to Ω_d^e, while CMB and LSS are more sensitive to Ω_d^e (and hence $\bar{\Omega}_{\rm ls}$ and $\bar{\Omega}_{\rm sf}$) than to the precise value of w_0.

where $R(a) \equiv \ln(\Omega_d(a)/[1-\Omega_d(a)])$ obeys

$$R(a) = R_0 - \frac{3w_0 \ln a}{1 - b \ln a}. \tag{2}$$

The constant b is fully specified by the three parameters w_0, Ω_d^0 and Ω_d^e:

$$b = -3w_0 \left(\ln \frac{1-\Omega_d^e}{\Omega_d^e} + \ln \frac{\Omega_d^0}{1-\Omega_d^0} \right)^{-1}. \tag{3}$$

In terms of w_0 and b, the equation of state is $w(a) = w_0/(1-b\ln a)^2$. For a comparison of our model to a cosmological constant, see figures 2 and 5. The advantage of a parameterization in terms of only three parameters is a minimal setting that accounts for information beyond a Taylor expansion around $z = 0$ (i.e. beyond the parameters Ω_d^0 and w_0). Nevertheless, it embodies the most crucial potential new feature of a dynamical dark energy, namely the possibility of early dark energy. For supernovae, it seems more suitable than a continuation of the Taylor expansion which at the next step involves the derivative of the equation of state $w_0' = \partial w/\partial z\,|_{z=0}$. The present bounds on w_0' [1] allow a region of large $|w_0'|$ for which the validity of a Taylor expansion is doubtful even for $z = 1$.

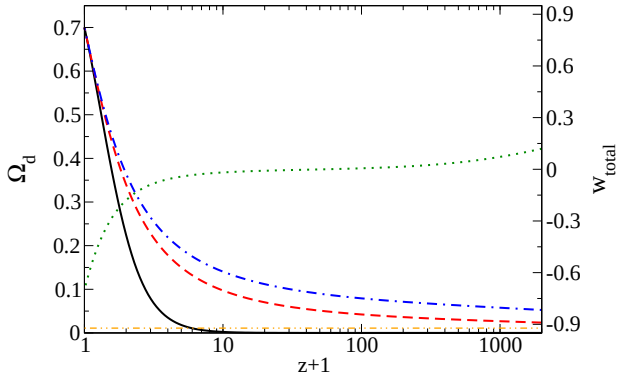

FIG. 2: Evolution of a typical dark energy model considered in this paper with $\Omega_d^0 = 0.7$, $w_0 = -0.999$ and $\Omega_d^e = 0.01$ depicted as dashed (red) line and with $\Omega_d^e = 0.03$ depicted as dashed-dotted (blue) line. These two models correspond to values of Ω_d^e that are allowed within 1σ and 2σ respectively. For comparison, the solid (black) line shows the evolution for a cosmological constant with same Ω_d^0. The straight dashed-double dotted (orange) line at $\Omega_d = 0.01$ indicates the asymptotic limiting value of Ω_d for our model with $\Omega_d^e = 0.01$. In contrast to the cosmological constant which contributes negligible at early times, our models have $\Omega_d \geq 0.01$ (0.03) always and contribute a considerable effective fraction $\bar{\Omega}_{\rm sf} \sim 0.06$ (0.1) during structure formation. The dotted (green) line indicates the total equation of state of the Universe for our $\Omega_d^e = 0.01$ model. For $w_{total} < -1/3$, the Universe is accelerating.

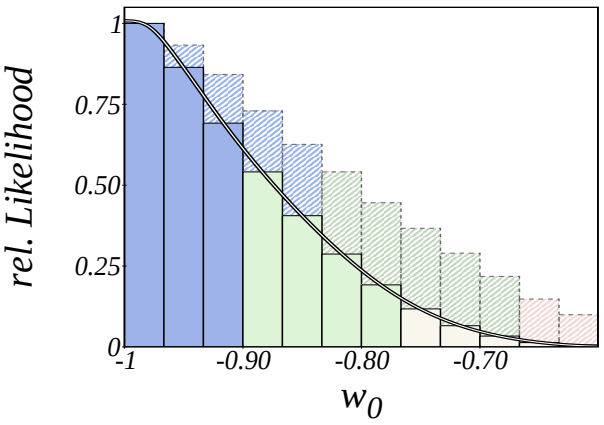

FIG. 3: Constraints on the equation of state today. The dark (blue), medium (green) and light (red) shaded regions correspond to $1, 2$ and 3σ confidence. The constraints from Sne Ia is displayed in the foreground (solid), while the less tight constraint from WMAP+CBI+VSA+SDSS+HST is depicted in the background.

In addition to the dark energy parameters Ω_d^0, w_0 and Ω_d^e, we consider the matter and baryon densities today $\Omega_m^0 h^2$ and $\Omega_b^0 h^2$, the Hubble parameter h, optical depth to the last scattering surface τ and spectral index n.

We compare the predictions of these models to the Sne Ia data of [1] , as well as to the data from WMAP [2], CBI [3], VSA [5], SDSS [6] and the Hubble parameter constraint of the Hubble Space Telescope [8] combined. For this, we employ the AnalyzeThis! [21] Monte Carlo package of cmbeasy [22]. We ran simulations both in terms of Ω_d^e, Ω_d^0 and w_0 as well as in terms of b, Ω_d^0 and w_0, i.e we computed chains where the parameter Ω_d^e is traded for the parameter b and vice versa. For a constraint on the parameter b from WMAP and Sne Ia, see Figure 4.

As far as the model parameters w_0 and Ω_d^e are concerned, the main results are encapsulated in Figures 1, 3 and 6. As is seen from Figure 1, the information provided by CMB plus LSS and Sne Ia are almost orthogonal. While Sne Ia restrict w_0 considerably better than CMB and LSS combined, the sensitivity to Ω_d^e is worse. From Sne Ia, we find $w_0 < -0.78$, while $\Omega_d^e < 0.029$ from CMB, LSS and HST.

The average dark energy fractions at last scattering and during structure formation, $\bar{\Omega}_{\rm ls}$ and $\bar{\Omega}_{\rm sf}$ can substantially deviate from Ω_d^e (as seen in Figures 9 and 10). As the underlying probability density is unknown, we cannot quote constraints on $\bar{\Omega}_{\rm ls}$ and $\bar{\Omega}_{\rm sf}$ from counting the number of models in the chain per bin. Instead, we choose to draw the distribution of the maximum likelihood model per bin. Figures 9 and 10 show this distribution. The somewhat tight $2-\sigma$ constraint on $\bar{\Omega}_{\rm ls}$ is a result of our parameterization: the amount of dark energy during structure formation $\bar{\Omega}_{\rm sf}$ always exceeds $\bar{\Omega}_{\rm ls}$. As the ISW effect in the CMB anisotropies as well as effects on the cold dark matter power spectrum restrict $\bar{\Omega}_{\rm sf} \lessapprox 10\%$, this leads to $\bar{\Omega}_{\rm ls} \lessapprox 5\%$ at 95% confidence level.

Models of early dark energy typically lead to slightly lower values of h than Λ-CDM. The reason is the CMB: dark energy influences the CMB mostly due to projection effects and additional ISW contributions. To match observations, any model must at least provide an acoustic scale l_A that comes close to the one measured by WMAP. With Ω_d^0 fixed, the analytic expression for l_A of [17] yields

$$l_A \propto \int_0^1 {\rm d}a \left(a + \frac{\Omega_d^0}{1-\Omega_d^0}\, a^{(1-3\bar{w})} + \frac{\Omega_r^0 (1-a)}{1-\Omega_d^0} \right)^{-1/2}, \quad (4)$$

where Ω_r is the present energy fraction in radiation and $\bar{w}$ is the weighted average

$$\bar{w} = \int_0^{\tau_0} \Omega_d(\tau) w(\tau) {\rm d}\tau \times \left(\int_0^{\tau_0} \Omega_d(\tau) {\rm d}\tau \right)^{-1}. \quad (5)$$

The integral (4) increases when $\bar{w} \to -1$, i.e. for all other parameters fixed, the acoustic scale l_A becomes larger the more negative $\bar{w}$. Conversely, as our models have $\bar{w} > -1$ by construction, we see that for all other parameters fixed, our models have a smaller acoustic scale compared to Λ-CDM. To counterbalance this, a somewhat smaller Hubble parameter h is preferred (see Figure 7), because

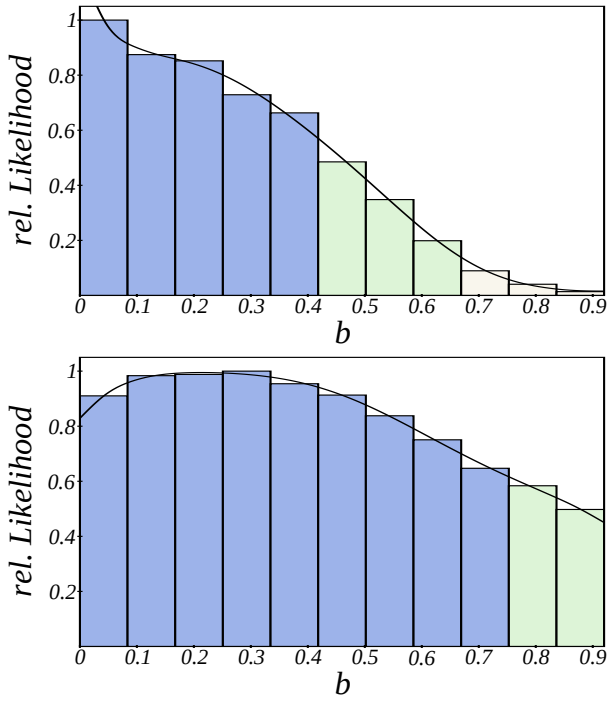

FIG. 4: Constraints on the parameter b from WMAP+CBI+VSA+SDSS+HST data (upper panel) and Sne Ia (lower panel).The dark (blue), medium (green) and light (red) shaded regions correspond to $1, 2$ and 3σ confidence.

l_A depends on h to good approximation as [17]

$$l_A \propto 1 + h^{-1}\sqrt{\frac{\Omega^0_{rel.}h^2}{a_{ls}(1-\Omega^0_d)}} \approx 1 + 0.4h^{-1}, \qquad (6)$$

where we have used the estimates $\Omega^0_d \approx 0.7$, $a_{ls} \approx 1100^{-1}$ and $\Omega^0_{rel.}h^2 \approx 4.4 \times 10^{-5}$. Likewise, a sizeable early dark energy $\bar{\Omega}_{\rm ls}$ can increase the acoustic scale according to $l_A \propto 1/\sqrt{1-\bar{\Omega}_{\rm ls}}$ [17]. Both $\bar{\Omega}_{\rm ls}$ and the somewhat smaller Hubble parameter counterbalance the effect of $\bar{w}$ in our models.

Just as $\bar{\Omega}_{\rm ls}$ expresses the main effect of early dark energy on the CMB, the suitable average

$$\bar{\Omega}_{\rm sf} = [\ln a_{tr.} - \ln a_{eq.}]^{-1} \int_{\ln a_{eq.}}^{\ln a_{tr.}} \Omega_d(a)\, {\rm d}\ln a \qquad (7)$$

with $a_{tr.} = 1/3$ encapsulates main effects of early dark energy on structure formation [18]. By definition, one has $\bar{\Omega}_{\rm sf}(\Lambda) \sim 0.5\%$ (i.e. non-vanishing) for a cosmological constant model and our choice of $a_{tr.}$. A sizeable $\bar{\Omega}_{\rm sf}$ leads to a decrease in linear structure compared to Λ-CDM according to [18]

$$\frac{\sigma_8(D.E.)}{\sigma_8(\Lambda)} \propto a_{eq.}^{3\bar{\Omega}_{\rm sf}/5} \qquad (8)$$

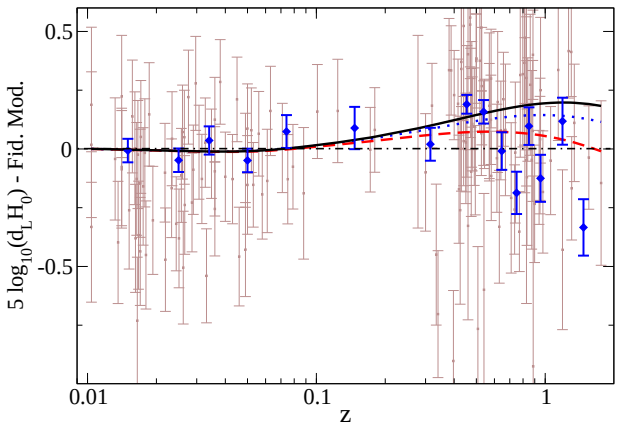

FIG. 5: Supernovae compilation of Riess et. al. [1] as data points with thin (brown) error bars. In addition we plot the same data in binned fashion for illustration purposes [24]. We plot the logarithm of the luminosity distance minus a fiducial model for which $d_L H_0 = (1+z)\ln(1+z)$. The solid (black) line is for a cosmological constant model, the dotted (blue) line is for $\Omega^e_d = 10^{-4}$ and the dashed (red) line is for $\Omega^e_d = 10^{-1}$. All models have $w_0 = -1$ in common.

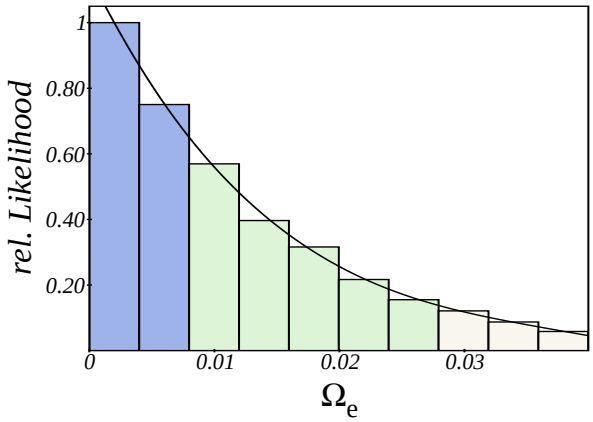

FIG. 6: Likelihood distribution of the early dark energy parameter Ω^e_d inferred from WMAP+CBI+VSA+SDSS+HST data. The dark (blue), medium (green) and light (red) shaded regions correspond to $1, 2$ and 3σ confidence.

Using $z_{eq.} = 3500$, we obtain for $3\bar{\Omega}_{\rm sf} \ln z_{eq.}/5 \ll 1$, the quick estimate

$$\frac{\sigma_8(D.E.)}{\sigma_8(\Lambda)} \propto (1 - 6\,[\bar{\Omega}_{\rm sf} - \bar{\Omega}_{\rm sf}(\Lambda)]), \qquad (9)$$

As we leave a free bias for our SDSS analysis, and have no prior on σ_8, one may worry about unphysically low values of σ_8 for our models. It does turn out, however, that this is not necessarily the case. As seen in Figure 8, our predictions for σ_8 are compatible with observations, given the lower values of σ_8 needed to explain non-linear structure in early dark energy scenarios compared to ΛCDM [23].

Cosmological probes have reached a level of accuracy

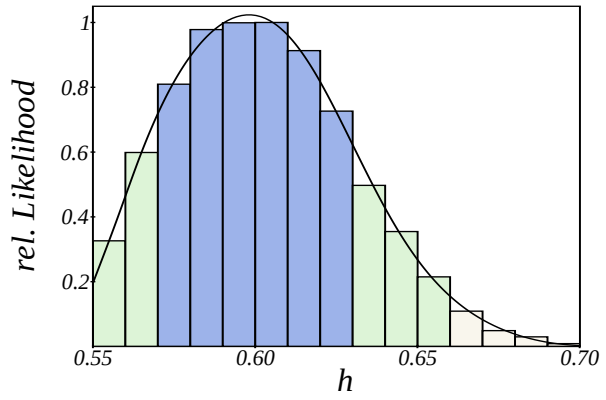

FIG. 7: Likelihood distribution for the hubble parameter h yielding $h = 0.6 \pm 0.03$. As explained in the text, slightly lower values of h than in standard ΛCDM models are preferred. The data used was WMAP+CBI+VSA+SDSS+HST.

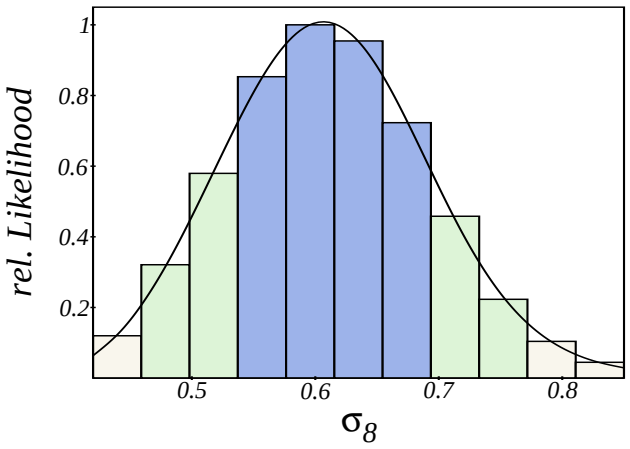

FIG. 8: The linear rms power of matter fluctuations on $8h^{-1}$Mpc scales, σ_8. As σ_8 is not a monte carlo parameter, we caution the reader that the underlying prior is not flat. With $\sigma_8 = 0.61 \pm 0.08$ the power is rather low compared to a standard Λ CDM model – a direct result of the suppression of growth due to the presence of dark energy during structure formation.

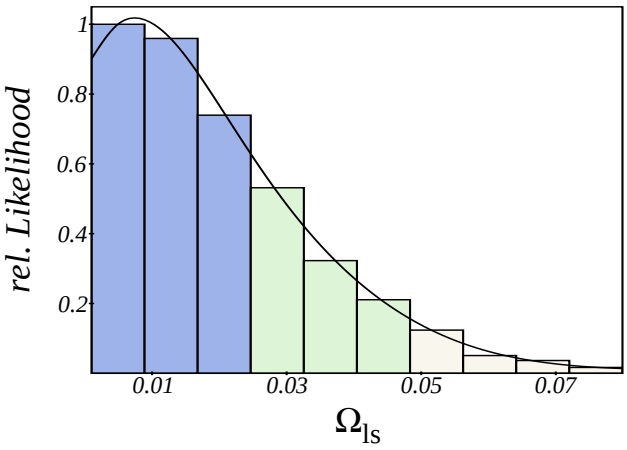

FIG. 9: The average dark energy contribution during structure formation $\bar{\Omega}_{\rm ls}$ as defined in Equation (7). As $\bar{\Omega}_{\rm ls}$ is not a monte carlo parameter, but a derived quantity, we plot the maximum likelihood of all models per bin. In the model considered, we see that a model with overall Likelihood less than $\Delta\chi^2 = 1$ apart from the best fit model can be found only for $\bar{\Omega}_{\rm ls} \lesssim 3\%$.

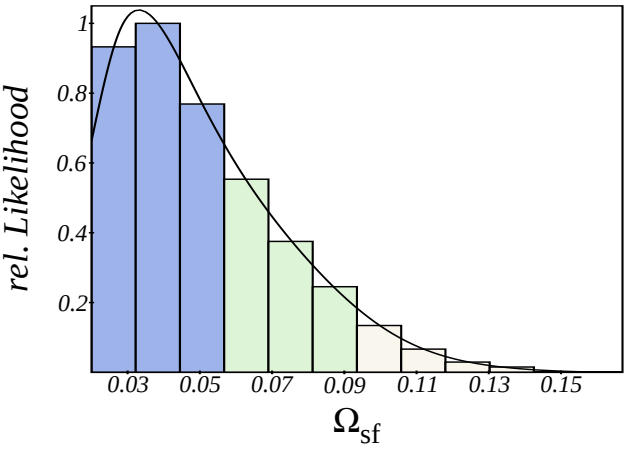

FIG. 10: The average dark energy contribution during structure formation $\bar{\Omega}_{\rm sf}$ as defined in Equation (7). As $\bar{\Omega}_{\rm sf}$ is not a monte carlo parameter, but a derived quantity, we plot the maximum likelihood of all models per bin. Please note that $\bar{\Omega}_{\rm sf} \sim 0.5\%$ by definition even for a cosmological constant Universe.

that leads to stringent constraints on any model of our Universe. In the case of the parameterization of dark energy in terms of Ω_d^0, Ω_d^e and w_0 we used, the Supernovae Ia and CMB+LSS experiments provide almost orthogonal information. From the background evolution at $z \lesssim 2$ that are probed by current Sne Ia observations, we find $w_0 \lesssim -0.78$ at 95 % confidence level, in good agreement with prior investigations (e.g. [25, 26]). Likewise, structure formation and the cosmic microwave background yield strong bounds on the abundance of dark energy at very high redshift. In our model, $\Omega_d^e < 0.029$ at 95% confidence level. The value of Ω_d^e is a factor of $2-3$ lower than the abundance of dark energy allowed during recombination $\bar{\Omega}_{\rm ls}$ and the abundance during structure formation $\bar{\Omega}_{\rm sf}$. This is both a feature and a shortcoming of our simple parameterization. Curing it would require more parameters which at the present time are not necessary to explain current observations. As early dark energy models such as the one investigated in this paper make clear predictions for the CMB and in particular for structure formation, it will become possible to falsify or confirm such a scenario within the not so distant future. In this regard, the model investigated here holds more opportunities for detection than models of dark energy with negligible Ω_d at higher redshifts.

[1] A. G. Riess *et al.* [Supernova Search Team Collaboration], Astrophys. J. **607**, 665 (2004) [arXiv:astro-ph/0402512].

[2] D. N. Spergel *et al.* [WMAP Collaboration], Astrophys. J. Suppl. **148**, 175 (2003) [arXiv:astro-ph/0302209].

[3] A. C. S. Readhead *et al.*, Astrophys. J. **609** (19??) 498 [arXiv:astro-ph/0402359].

[4] J. H. Goldstein *et al.*, Astrophys. J. **599**, 773 (2003) [arXiv:astro-ph/0212517].

[5] R. Rebolo *et al.*, arXiv:astro-ph/0402466.

[6] M. Tegmark *et al.* [SDSS Collaboration], Phys. Rev. D **69** (2004) 103501 [arXiv:astro-ph/0310723].

[7] E. Hawkins *et al.*, Mon. Not. Roy. Astron. Soc. **346** (2003) 78 [arXiv:astro-ph/0212375].

[8] W. L. Freedman *et al.*, Astrophys. J. **553** (2001) 47 [arXiv:astro-ph/0012376].

[9] C. Wetterich, Nucl. Phys. B **302**, 668 (1988)

[10] B. Ratra and P. J. Peebles, Phys. Rev. D **37**, 3406 (1988)

[11] R. R. Caldwell, R. Dave and P. J. Steinhardt, Phys. Rev. Lett. **80**, 1582 (1998)

[12] R. R. Caldwell, Phys. Lett. B **545**, 23 (2002) [arXiv:astro-ph/9908168].

[13] P. S. Corasaniti and E. J. Copeland, Phys. Rev. D **67**, 063521 (2003) [arXiv:astro-ph/0205544].

[14] E. V. Linder, Phys. Rev. Lett. **90**, 091301 (2003).

[15] A. Upadhye, M. Ishak and P. J. Steinhardt, arXiv:astro-ph/0411803.

[16] Y. Wang and M. Tegmark, Phys. Rev. Lett. **92**, 241302 (2004) [arXiv:astro-ph/0403292].

[17] M. Doran, M. J. Lilley, J. Schwindt and C. Wetterich, Astrophys. J. **559**, 501 (2001) [arXiv:astro-ph/0012139].

[18] M. Doran, J. M. Schwindt and C. Wetterich, Phys. Rev. D **64**, 123520 (2001) [arXiv:astro-ph/0107525].

[19] R. R. Caldwell, M. Doran, C. M. Mueller, G. Schaefer and C. Wetterich, Astrophys. J. **591** (2003) L75 [arXiv:astro-ph/0302505].

[20] C. Wetterich, Phys. Lett. B **594**, 17 (2004) [arXiv:astro-ph/0403289].

[21] M. Doran and C. M. Mueller, J. Cosmol. Astropart. Phys. JCAP09(2004)003 [arXiv:astro-ph/0311311].

[22] M. Doran, arXiv:astro-ph/0302138.

[23] M. Bartelmann, M. Doran and C. Wetterich, arXiv:astro-ph/0507257.

[24] B. Leibundgut, private communication.

[25] H. K. Jassal, J. S. Bagla and T. Padmanabhan, Mon. Not. Roy. Astron. Soc. **356** (2005) L11 [arXiv:astro-ph/0404378].

[26] S. Hannestad and E. Mortsell, Phys. Rev. D **66** (2002) 063508 [arXiv:astro-ph/0205096].